Published in final edited form as:
Nanomedicine. 2010 June ; 6(3): 442–452. doi:10.1016/j.nano.2009.10.005.

Novel cationic fullerenes as broad-spectrum light-activated antimicrobials

Liyi Huang, PhD[1,2,3], **Mitsuhiro Terakawa, PhD**[1,4], **Timur Zhiyentayev, MS**[1,5], **Ying-Ying Huang, MD**[1,2,6], **Yohei Sawayama, BS**[1,7], **Ashlee Jahnke, BS**[8], **George P Tegos, PhD**[1,2], **Tim Wharton, PhD**[8], and **Michael R Hamblin, PhD**[1,2,9,*]

[1] Wellman Center for Photomedicine, Massachusetts General Hospital, Boston, MA

[2] Department of Dermatology, Harvard Medical School, Boston, MA

[3] Department of Infectious Diseases, First Affiliated College & Hospital, Guangxi Medical University, Nanning, China

[4] Department of Electronics and Electrical Engineering, Keio University, Japan

[5] Chemistry Department, Massachusetts Institute of Technology, Cambridge, MA

[6] Aesthetic and Plastic Center, Guangxi Medical University, Nanning, China

[7] Graduate School of Engineering, University of Tokyo, Japan

[8] Lynntech Inc, College Station, TX

[9] Harvard-MIT Division of Health Sciences and Technology, Cambridge, MA

Abstract

Photodynamic inactivation (PDI) is a rapidly developing antimicrobial technology which combines a non-toxic photoactivatable dye or photosensitizer (PS) in combination with harmless visible light of the correct wavelength to excite the dye to its reactive triplet state that will then generate reactive oxygen species (ROS) that are highly toxic to cells. Buckminsterfullerenes are closed-cage molecules entirely composed of *sp2* hybridized carbon atoms and although their main absorption is in the UV, they also absorb visible light and have a long-lived triplet state. When C60 fullerene is derivatized with cationic functional groups it forms molecules that are more water-soluble and can mediate PDT efficiently upon illumination, and moreover cationic fullerenes can selectively bind to microbial cells. In this report we describe the synthesis and characterization of several new cationic fullerenes. Their relative effectiveness as broad-spectrum antimicrobial photosensitizers against Gram-positive, Gram-negative bacteria, and a fungal yeast was determined by quantitative structure function relationships.

[*]Corresponding author: Michael R Hamblin, PhD, 40 Blossom Street, BAR414, Wellman Center for Photomedicine, Massachusetts General Hospital, Boston, MA 02114-2696, Phone: (617) 726-6182, Fax: (617) 726-6182, hamblin@helix.mgh.harvard.edu.

Conflict of Interest Statement.
Ashlee Jahnke and Tim Wharton are employees of Lynntech Inc, a company with interests in fullerene synthesis. Tim Wharton and Michael R Hamblin are inventors on a patent for antimicrobial PDT with cationic fullerenes.

Keywords

Photodynamic therapy; functionalized fullerenes; antimicrobial photoinactivation; quantitative structure function relationships; broad-spectrum antimicrobials

Introduction

There has been a relentless rise in antibiotic resistance that has taken place over many years in most regions of the world and has been observed in many different classes of microbial cells (1). In recent times the phenomenon has become even more worrying, with concerns that hitherto fairly trivial infections could again become untreatable as in the days before antibiotics were discovered (2). In fact the present time has been referred to as the “end of the antibiotic era” (3). The rise in multidrug resistance amongst microbial pathogens has motivated an international search for alternative antimicrobial strategies, particularly those which could be applied to infections in wounds and burns.

Photodynamic therapy (PDT) employs a nontoxic dye termed a photosensitizer (PS) and low-intensity visible light, which in the presence of oxygen produce reactive oxygen species (ROS), such as singlet oxygen, superoxide and hydroxyl radical (4). PDT has the advantage of dual selectivity in that the PS can be targeted to its destination cell or tissue, and in addition the illumination can be spatially directed to the lesion. PDT was originally discovered over a hundred years ago by its light-mediated killing effect on microorganisms (5), but since then has been principally developed as a treatment for cancer (6) and age-related macular degeneration (7). PDT has recently attracted attention as a possible alternative treatment for localized infections (8-10). It is proposed that for antimicrobial PDT the PS would be topically or locally applied to the infected tissue and, after a relatively short time interval, light would be delivered to the area and depending on the effectiveness of the antimicrobial PS, up to three logs of bacterial or fungal cells would be killed without causing unacceptable damage to the host tissue. A three-log reduction is accepted as an effective antimicrobial intervention equivalent to disinfectants (11). It has been reported that PDI is equally effective (12) (or even more effective (13)) against multi-drug resistant bacteria as it was against naïve species, and moreover, the PDI treatment itself is considered to be unlikely to cause bacterial resistance to damage by ROS to arise (14). This is because the PDI insult is relatively brief (many logs killed over minutes) compared to antibiotics that are typically present for many days or weeks, and because the type of damage to bio-molecules done by PDT is relatively non-speciific compared to antibiotics that in general specifically inhibit a target enzyme.

It is known that Gram-negative bacteria are resistant to PDI with many commonly used PS that will readily lead to phototoxicity for Gram-positive species (15) and that PS bearing a cationic charge (16) or the use of agents that increase the permeability of the outer membrane will increase the efficacy of killing of gram-negative organisms (17). The ideal PS for killing bacteria should possess an overall cationic charge and preferably multiple cationic charges (18).

Buckminsterfullerenes are closed-cage molecules entirely composed of *sp2* hybridized carbon atoms. The presence of many conjugated double bonds gives these molecules a high optical absorption in visible wavelengths and a high triplet yield from the excited singlet state (19). The triplet state of the fullerene molecule can interact with molecular oxygen via two reaction pathways (Figure 1). Firstly energy transfer can take place between the fullerene triplet and ground state triplet oxygen giving the reactive species singlet oxygen (Type II pathway) and the ground state fullerene. Secondly, either the triplet fullerene (or possible the excited singlet fullerene) can accept an electron from a biological reducing agent such as nicotinamide adenine

dinucleotide reduced form (NAD(P)H) to give the fullerene radical anion. This species can then transfer an electron to molecular oxygen to form superoxide radical anion and restoring the fullerene ground state. Superoxide anion can subsequently give rise to hydrogen peroxide and the highly reactive hydroxyl radical (20). Although pristine C60 in the form of nanoaggregates (21) or cyclodextrin complexes (22) is able to produce ROS upon illumination, the process is more efficient in biological media when the fullerenes have been chemically derivatized to make them water soluble. We have previously shown that fullerenes derivatized with one or more cationic charges via quaternary ammonium groups efficiently bind and penetrate all classes of microbial cells, and therefore act as broad-spectrum light-activated antimicrobials (23). In this report we describe the preparation and testing of new functionalized fullerene-derivatives with cationic charges as broad-spectrum antimicrobial PS against a panel of human pathogens.

Materials and Methods

Fullerene synthesis and characterization

The compounds were characterized by ^{1}H and ^{13}C NMR, 500 MHz (Innova500 spectrometer), FTIR (ATR), and mass spectrometry (MALDI-TOF).

BF1: C_{60} (100 mg, 0.14 mmol) was dissolved in 150 mL toluene. Sarcosine (30.82 mg, 0.35 mmol) and 4-pyridinecarboxaldehyde (46 μL, 0.59 mmol) were added and the reaction mixture was refluxed for 48 h. The toluene was removed and the product dried overnight in vacuo. The product was purified on a silica gel column using a solvent ratio of 1000:1:1 of toluene, triethylamine, and ethyl acetate, respectively. MALDI TOF-MS calculated for $C_{68}H_{10}N_2$ 854.8, found 853.2 $[M-H]^-$. The brown powder was treated with a large excess of iodomethane at ambient temperature for 48 h. The material was collected by filtration and washed with methanol.

ESI-MS calculated for $C_{69}H_{13}N_2$ 869.4 $[M]^+$, found 869.1

^{1}H NMR (DMSO-d_6, TMS ref.) δ = 2.759 (3H, s), 4.352 (3H, s), 4.437 (1H, d), 5.161 (1H, d), 5.553 (1H, s), 8.593 (2H, d), 9.047 (2H, d)

^{13}C NMR (DMSO-d_6, TMS ref.) δ = 48.48, 69.09, 69.93, 76.53, 79.84, 126.0, 128.2, 128.9, 129.6, 136.0, 136.2, 137.0, 138.0, 139.6, 140.1, 140.3, 140.4, 141.8, 141.9, 143.3, 144.5, 144.7, 145.0, 145.3, 145.5, 145.6, 145.7, 145.8, 145.9, 146.1, 146.3, 146.5, 146.8, 147.4, 147.5, 151.8, 152.7, 154.3, 156.2, 156.6.

FT-IR ν (cm^{-1}): 2919, 1454, 1210, 1006, 739, 520

Log K_{OW} = -1.331

BF2 (mixture of bis and tris adduct): C_{60} (100 mg, 0.14 mmol) was dissolved in 50 mL chlorobenzene and the solution degassed with N_2 for 30 minutes. Piperazine-2-carboxylic acid dihydrochloride (84.6 mg, 0.42 mmol) in methanol (3 mL) and triethylamine (300 μL) was added followed by 4-pyridinecarboxaldehyde (52.4 μL, 0.56 mmol) and the reaction was refluxed for 48 h under N_2. The solvent was removed in vacuo, then the solid was dissolved in 10 mL methanol and 20 mL chloroform and loaded onto a silica gel column. The column was eluted with chloroform followed by chloroform:methanol:triethylamine (94:3:3) to remove the mono adducts. The remaining column material was then extracted with methanol to obtain the pure product precursors. The material was dissolved in 10 mL chloroform and treated with 3.0 mL iodomethane for 1 h followed by the addition of 10 mg K_2CO_3 and stirring

at ambient temperature for 24 h. After filtration, the product was washed with chloroform and dried *in vacuo* to give a brown solid.

FT-IR ν (cm^{-1}): 2922, 1454, 1210, 1008, 737

Log K_{ow} = -3.02

Synthesis of N-hexylglycine: N-hexylamine (2 mL, 15.2 mmol) was dissolved in ethanol (1.43 mL) and water (686 μL) and stirred in an ice bath. Iodoacetic acid (649 mg, 3.49 mmol) was added slowly and the reaction mixture was allowed to stand overnight at room temperature. The reaction mixture was added to acetone (50 mL) and placed in the fridge. The resulting white precipitate was recrystallized using methanol/acetone. The resulting white crystals were dried overnight at 40 °C under vacuum.

Synthesis of BF3, BF4, and BF5: C_{60} (264.6 mg, 0.367 mmol) was dissolved in 130 mL toluene. N-hexylglycine (117 mg, 0.735 mmol) and paraformaldehyde (55 mg, 1.84 mmol) were added and the solution was refluxed for 2 h. After solvent removal, product was re-dispersed in minimal toluene and loaded onto a silica gel column. Elution with toluene gave unreacted C_{60} followed by monoadduct and then two bands corresponding to bisadduct regioisomers of increasing polarity. The fractions were methylated at room temp for 4 days with a large excess of methyl iodide. **BF3** 31.6 mg, **BF4** 29.9 mg, **BF5** 39.1 mg. ESI MS calculated for $C_{69}H_{20}N$ 862.8 $[M]^+$, found 862.2 for **BF3**, calculated. for $C_{78}H_{40}N_2$ 502.4 $[M]^{2+}$, found 502.2 for **BF4 and BF5** (regioisomers).

BF3 ^{1}H NMR (TMS ref.) δ = 0.95 (t, 3H) 1.20-1.59 (bm, 8H), 2.19 (bm, 2H), 4.14 (s, 3H), 4.22 (b, 2H), 5.68 (d, 2H), 5.82 (d, 2H)

^{13}C NMR (TMS ref.) δ = 14.63, 22.59, 23.72, 26.24, 31.39, 48.50, 66.17, 69.21, 72.30, 136.2, 140.1, 140.2, 141.8, 142.4, 142.9, 143.0, 144.6, 144.7, 145.5, 145.7, 145.9, 146.3, 146.6, 147.6, 152.5, 153.3

FT-IR ν (cm^{-1}): 2920, 1245, 741, 572

Log K_{ow} = 0.542

BF4 and BF5 ^{1}H NMR (TMS ref.) δ = 0.95 (bm), 1.15-1.61 (bm), 2.15 (bm), 3.8-4.2 (m) 5.45-5.95 (m)

FT-IR ν (cm^{-1}): 2925, 1454, 1213, 1010, 738

BF4: Log K_{ow} = 0.184

BF5: Log K_{ow} = -0.440

LogP values—The measured logK_{ow} values were determined by dissolving a few milligrams of each compounds in 100 μL dimethlysulfoxide followed by dilution in 10 mL deionized water. The solution was shaken vigorously for > 1 h with 10 mL of n-octanol (equilibrium was established by extended shaking times). After allowing the phases to separate, each was analyzed by absorption spectroscopy at 405 nm and a ratio of the concentration in each phase determined. The calculated logP values were found using ACD/LogP DB software version 12.0 (ACD/Labs, Toronto, Ontario, Canada).

Microbial strains and culture conditions

The following microbial strains were used: *Staphylococcus aureus* 8325-4, *Escherichia coli* K12 and *Pseudomonas aeruginosa* (ATCC 19660), as well as the DAY286 reference strain (24) of *Candida albicans* (a gift from Aaron Mitchell, Department of Microbiology, Columbia University, New York, NY). Planktonic bacterial cells were cultured in brain-heart infusion (BHI) with aeration at 37°C in mid-log growth phase (unless otherwise stated). Cell numbers were estimated by measuring the OD at 600-nm (OD of 0.5 = 10^8 cells/mL). Yeasts were cultured in yeast peptone dextrose (YPD) with aeration at 30°C and cell number was assessed with a hematocytometer (25).

Photodynamic inactivation studies and CFU determination

Cells were grown overnight at 37°C (30°C for Candida) and refreshed for 2-4 hours before being collected through centrifugation and suspended in phosphate-buffered saline (PBS). A cell suspension consisting of 10^8 cells/mL for bacteria (10^7 cells/mL for Candida (26) was incubated with various concentrations of the BF compounds for 30 min at room temperature in the dark. 1 mL aliquots were transferred to a 24 well plate and illuminated at room temperature with a broad-band white light source (400-700-nm band pass filter, Lumacare, Newport Beach, CA) to deliver 10 J/cm^2 at an irradiance of 100 mW/cm^2 as measured with a power meter (Coherent). Cells treated with BF in the dark were incubated covered with aluminum foil for the same time as the PDT groups (30 min) At the completion of illumination (or dark incubation) aliquots (100 μl) were taken from each well to determine CFU. The aliquots were serially diluted 10-fold in PBS to give dilutions of 10^{-1} to 10^{-5} times in addition to the original concentration and 10 μl aliquots of each of the dilutions were streaked horizontally on square BHI or YPD (Candida) plates by the method of Jett and colleagues (27). Plates were streaked in triplicate and incubated for 12-36 h at 30°C or 37°C in the dark to allow colony formation.

A control group of cells treated with light alone (no BF added) showed the same number of CFU as absolute control (data not shown). Survival fractions were routinely expressed as ratios of CFU of microbial cells treated with light and BF (or BF in the absence of light) to CFU of microbes treated with neither.

Results

Synthesis and characterization of fullerenes

The newly reported fullerene derivatives whose structures are shown in Figure 2 were designed to be amphiphilic in nature. In previous work, we (23) and others (28) have shown that the presence of one or more cationic charges greatly increases the antimicrobial photoinactivation efficacy of fullerene based PS. The charge increases the association of PS with negatively charged pathogen membranes while the hydrophobic character increases association with and/or penetration into the lipid components of the membrane. The compounds were designed to increase either the lipophilic or the cationic character of previously synthesized compounds for comparison. Compounds **BF1-2** were designed to increase cationic charge per addend, while compounds **BF3-5** were designed to increase overall lipophilicity of the PS. The syntheses were based on the fulleropyrrolidine construct, first developed by Prato, *et. al.* (29). By column chromatography, the monosubstituted addend was collected as the first eluting brown band. However, by simple chromatography, the bis- and tris- mixture always co-eluted under all tested conditions. Thus, **BF2**, is a mixture of bis- and tris- substitution ratios. Based on multiple consistent mass spec analyses, it is estimated that the mixture is ~3:1 bis:tris. Monoadduct **BF3** eluted first on the column followed by two bands of regioisomeric bis-product in order of increasing polarity, **BB4-5**.

LogP values

The correlation between measured (mLogP) and calculated (cLog P) values is shown in Figure 3A. The R value is 0.9825 which was surprisingly high considering that cLogP is approximately eight orders of magnitude higher than mLogP. It is known that highly hydrophobic compounds (such as fullerenes) tend to aggregate in polar solvents, and this process of individual molecules aggregating in water makes actual logP measurements unreliable (30) and explains why there was such a large difference between mLogP and cLogP. Aggregates and clusters of the hydrophobic compounds are solid-state particles and the logP definition loses its validity because the system contains both individual molecules and aggregates. The linear correlation between mLogP (aggregates, individual molecules) and cLogP (assuming that there are only individual molecules) implies that the effect of aggregation on logP depends on the difference in polarity of the two solvents and not on the relative hydrophobicities of the molecules. There was also a good linear correlation of 0.92 between cLogP and the number of cationic charges (Figure 3B) as might be expected considering the rest of the fullerene molecules (and the hydrophobicity attributed to the side-chain functionality) remains relatively similar.

Antimicrobial photoinactivation

The best way to compare PDT efficiencies of different fullerene molecules is to vary the fullerene concentration while keeping the light fluence constant either as dark (0 J/cm^2) or as 10 J/cm^2. We studied the PDT effects on Gram-positive bacteria (*S. aureus*), two different Gram-negative bacteria (*E. coli* and *P. aeruginosa*) and a fungal yeast *C. albicans*.

Figure 4 shows the killing curves for **BF1** against the four microbial species. *S. aureus* (Figure 4A) was most susceptible with 1 μM **BF1** giving complete eradication and only modest (1.5 log) dark toxicity. *E coli* (Figure 4B) was next most susceptible with over 5 logs of killing at 10 μM **BF1** and three logs of dark toxicity. *P aeruginosa* (Figure 4C) and *C. albicans* (Figure 4D) were least susceptible with 4 and 5 logs of killing at 100 μM respectively and considerable dark toxicity (2 and 4 logs respectively).

Figure 5 shows that **BF2** was overall the most powerful of the five fullerenes tested. More than 3 logs of *S. aureus* (Figure 5A) was killed at the surprisingly low concentration of 100 nM with no dark toxicity, and cells were eliminated at 1 μM. *E. coli* (Figure 5B) was eliminated at 10 μM with three logs of dark toxicity. In the case of **BF2**, *P. aeruginosa* (Figure 5C) was more susceptible to PDT than *E. coli* with over 4 logs of killing at 1 μM with no dark toxicity and elimination at 10 μM. *C. albicans* (Figure 5D) had over 5 logs of killing at 10 μM and was eliminated at 100 μM with considerable (over 5 logs) dark toxicity.

BF3 (Figure 6) was the least effective PS of those fullerenes tested. Three logs of *S. aureus* was killed at 1 μM (Figure 6A) and 3 logs of *E. coli* was killed at 100 μM (Figure 6B) without dark toxicity, while no *P. aeruginosa* (Figure 6C) or *C. albicans* (Figure 6D) was killed at the concentrations tested.

BF4 (Figure 7) was somewhat more effective than **BF3**. More than 3 logs of *S. aureus* (Figure 7A) was killed at 1 μM and *E. coli* (Figure 7B) was eliminated at 100 μM. There was modest killing of *P aeruginosa* (Figure 7C) at 100 μM and in all three cases dark toxicity was moderate. No *C. albicans* was killed with either **BF4** or **BF5** at concentrations up to 100 μM (data not shown).

BF5 (Figure 8) was more effective than either **BF3** or **BF4**. *S. aureus* (Figure 8A) was killed 3.5 logs at 1 μM; *E. coli* (Figure 8B) was killed 5 logs at 100 μM and *P. aeruginosa* (Figure 8C) was killed 3 logs at 100 μM, with dark toxicity only apparent in the case of *E. coli*.

Quantitative structure function relationship (QSAR) correlations

We plotted the concentration of fullerenes necessary to kill 2 logs (LD99) of microbial cells (after illumination with 10 J/cm^2 of white light), against the calculated values of logP (Figure 9). Although all three microbial species gave extremely good exponential correlations, the correlation for *S. aureus* (Figure 9A) was the least good with R = 0.862. The correlation for *E. coli* (Figure 9B) gave a R value of 0.976, and the correlation for *P. aeruginosa* (Figure 9C) was almost perfect at R = 0.999. Therefore for these fullerenes their effectiveness as antimicrobial PS against both Gram-positive and Gram-negative bacteria negatively correlates with their calculated logP values.

Discussion

Functionalized fullerenes have several attractive features as antimicrobial PS (19). They have a high degree of photostability compared to tetrapyrrole-based PS, they tend to produce more Type I ROS such as hydroxyl radical and superoxide compared to alternative PS structures (20), and they show selectivity for microbial cells over mammalian cells (31). Fullerenes have been an important feature of the nanotechnology revolution (32). Although their molecular diameter is only of the order of 1 nm, they are generally accepted as nanoparticles, and their use as antimicrobial PS may be a real application of nanotechnology in medicine.

It is well known that cationic charges are a highly desirable feature in antimicrobial PS (33). It is usually considered that *S. aureus* as a typical Gram-positive bacterium is easily killed by PDT using PS of diverse molecular structures. The structure of the Gram-positive bacterial cell includes a relatively porous outer coat of peptidoglycan as well as polysaccharides and lipoteichoic acids that encircles a single cytoplasmic membrane composed of a lipid bilayer. Many dyes and PS of diverse structures and various overall molecular charges can bind and penetrate the Gram-positive cell wall. By contrast the Gram-negative bacterial structure is characterized by a double lipid bilayer encasing a thin layer of peptidoglycan, and it is accepted that this structure presents a much more effective permeability barrier to many classes of molecule than the Gram-positive bacterial cell wall structure.

The overall electrostatic charge borne by the outer surface of both classes of bacteria (Gram-positive and Gram-negative) is negative, and *E. coli* cells were reported to be the most negatively charged as measured by a zeta potential of − 16 mV, followed by *S. aureus* at − 10 mV and *P. aeruginosa* at − 7 mV (34). The other particular physical property of the different bacterial cells that is relevant to the binding of fullerene PS is the hydrophobicity. This is conveniently measured by the contact angle or wettability and *S. aureus* was reported to be the most hydrophobic at 72.2 deg, followed by *P. aeruginosa* at 43.3 deg and the most hydrophilic was *E. coli* at 33 deg (35).

The fact that *S. aureus* cells are most hydrophobic may explain why the negative correlation between fullerene logP value and PDT effectiveness for this species was the least good (Figure 9A). Because logP is negatively correlated with number of cationic charges in this series, and in general the number of cationic charges governs the binding of PS to bacteria, it would be expected that for hydrophilic bacterial cells like *P. aeruginosa* and *E. coli* the fullerene with the lowest logP value would be the best PS, but that hydrophobic *S. aureus* cells may bind fullerenes based on both cationic charge and on hydrophobicity, thus lessening the correlation. The QSAR studies showed a better correlation for LogP against *P. aeruginosa* than was found against *E. coli* (compare Figures 9B and 9C). The explanation for this is that cationic molecules are more suited to disrupting the outer-membrane lipolysaccharide in *P. aeruginosa* than in *E. coli* probably due to the greater role of divalent cations in the former case. It is thought that cationic molecules displace Ca^{++} and Mg^{++} and thereby weakening the outer structure (36).

Our previous study (23) on a series of three cationic fullerenes with 1, 2, and 3 cationic charges associated with dimethylpyrrolidinium groups demonstrated that increasing number of cationic charges correlated with increasing efficiency in light-mediated killing of Gram-positive bacteria (*S. aureus*) Gram-negative bacteria (*E. coli* and *P. aeruginosa*), and fungal yeast (*C. albicans*). The present study employed compounds with a wider range of different hydrophobicities, as well as an increased number of cationic charges (**BF2**). The finding that the effectiveness for antimicrobial PDT negatively correlates with hydrophobicity suggests that water solubility is important, and that drug-delivery vehicles that are necessary for hydrophobic more water insoluble compounds will not be needed if cationic fullerenes are used as clinical antimicrobial PS.

The extra permeability barrier characteristic of Gram-negative bacteria compared to Gram-positives is considered to be primarily against hydrophobic molecules (37). Small hydrophilic molecules tend to diffuse into bacteria via porin channels in Gram-negative species (38), but Yoshimura reported that even for hydrophilic molecules *P. aeruginosa* was 100 times less permeable than *E. coli* (39). *P. aeruginosa* is frequently considered to have high intrinsic antibiotic resistance due to its low outer membrane permeability (40). This intrinsic resistance is reflected in our finding that *P. aeruginosa* was the least susceptible of the three bacterial species tested to all the fullerenes except the polycationic **BF2**, where it was moderately susceptible.

The clear dependence of effectiveness of fullerene PS as anti-bacterial PS on the number of cationic charges may have two possible explanations. Firstly the amount of fullerene that binds to each negatively charged cell could be expected to depend on the number of positive charges on the molecule, and secondly the degree to which the outer membrane permeability barrier is breached by the self-promoted uptake pathway mediated by cationic molecules (41,42) may be expected to depend on the number of cationic charges.

In contrast to bacteria, much less is known about structure function relationships amongst PS that are effective against fungal yeasts such as Candida. PS such as Photofrin that is an approved PS against cancer has been used to kill Candida (43), while in other studies cationic phenothiazinium salts such as methylene blue (44) and toluidine blue (45) have been employed. Candida cells also have an overall negative charge and may have varying hydrophobicity depending to some extent on growth conditions (46,47). In the present study, only **BF2** (and to a lesser extent **BF1**) was effective in killing Candida and the ratio between PDT toxicity and dark toxicity was somewhat less that that found for bacterial cells.

In conclusion, cationic fullerenes were found to be highly active broad spectrum antimicrobial PS and represent a potential contribution of nanotechnology to medicine. QSAR relationships were established that indicated that increasing the number of cationic charges and lowering the hydrophobicity tended to increase the PDT efficiency against both Gram-positive and Gram-negative bacteria. Although not specifically studied in this report, previous findings from our (23,48) and other laboratories (49,50) have indicated that at the short incubation times (10-30 min) typically employed in antimicrobial PDT experiments, there is a high level of selectivity for of antimicrobial PS for microbial cells over mammalian cells because compounds like cationic fullerenes are only slowly taken up by the latter cell types by the time-dependent process of endocytosis. We have undertaken a study of fullerene mediated PDT against a small animal model of bacterial wound infection that will be reported separately.

Acknowledgments

Funding sources

This work was supported by NIH (grants R44AI068400 and R44CA103177 to TW and R01AI050875 to MRH).

References

1. Yoneyama H, Katsumata R. Antibiotic resistance in bacteria and its future for novel antibiotic development. Biosci Biotechnol Biochem 2006;70:1060–1075. [PubMed: 16717405]
2. Dowell SF. Antimicrobial resistance: is it really that bad? Semin Pediatr Infect Dis 2004;15:99–104. [PubMed: 15185193]
3. Yoshikawa TT. Antimicrobial resistance and aging: beginning of the end of the antibiotic era? J Am Geriatr Soc 2002;50:S226–229. [PubMed: 12121517]
4. Hamblin, MR.; Mroz, P. Advances in photodynamic therapy: basic, translational and clinical. Norwood, MA: Artech House; 2008.
5. Moan J, Peng Q. An outline of the hundred-year history of PDT. Anticancer Res 2003;23:3591–3600. [PubMed: 14666654]
6. Dolmans DE, Fukumura D, Jain RK. Photodynamic therapy for cancer. Nat Rev Cancer 2003;3:380–387. [PubMed: 12724736]
7. Wormald R, Evans J, Smeeth L, Henshaw K. Photodynamic therapy for neovascular age-related macular degeneration. Cochrane Database Syst Rev 2007:CD002030. [PubMed: 17636693]
8. Hamblin MR, Hasan T. Photodynamic therapy: a new antimicrobial approach to infectious disease? 2004;3:436–450.
9. Jori G, Brown SB. Photosensitized inactivation of microorganisms. Photochem Photobiol Sci 2004;3:403–405. [PubMed: 15122355]
10. Maisch T. Anti-microbial photodynamic therapy: useful in the future? Lasers Med Sci 2007;22:83–91. [PubMed: 17120167]
11. Lilly HA, Lowbury EJ, Wilkins MD. Limits to progressive reduction of resident skin bacteria by disinfection. J Clin Pathol 1979;32:382–385. [PubMed: 447872]
12. Soncin M, Fabris C, Busetti A, Dei D, Nistri D, Roncucci G, et al. Approaches to selectivity in the Zn(II)-phthalocyanine-photosensitized inactivation of wild-type and antibiotic-resistant Staphylococcus aureus. Photochem Photobiol Sci 2002;1:815–819. [PubMed: 12656484]
13. Tang HM, Hamblin MR, Yow CM. A comparative in vitro photoinactivation study of clinical isolates of multidrug-resistant pathogens. J Infect Chemother 2007;13:87–91. [PubMed: 17458675]
14. Lauro FM, Pretto P, Covolo L, Jori G, Bertoloni G. Photoinactivation of bacterial strains involved in periodontal diseases sensitized by porphycene-polylysine conjugates. Photochem Photobiol Sci 2002;1:468–470. [PubMed: 12659156]
15. Malik Z, Ladan H, Nitzan Y. Photodynamic inactivation of Gram-negative bacteria: problems and possible solutions. J Photochem Photobiol B 1992;14:262–266. [PubMed: 1432395]
16. Merchat M, Bertolini G, Giacomini P, Villanueva A, Jori G. Meso-substituted cationic porphyrins as efficient photosensitizers of gram-positive and gram-negative bacteria. J Photochem Photobiol B 1996;32:153–157. [PubMed: 8622178]
17. Nitzan Y, Gutterman M, Malik Z, Ehrenberg B. Inactivation of gram-negative bacteria by photosensitized porphyrins. Photochem Photobiol 1992;55:89–96. [PubMed: 1534909]
18. Alves E, Costa L, Carvalho CM, Tome JP, Faustino MA, Neves MG, et al. Charge effect on the photoinactivation of Gram-negative and Gram-positive bacteria by cationic meso-substituted porphyrins. BMC Microbiol 2009;9:70. [PubMed: 19368706]
19. Mroz P, Tegos GP, Gali H, Wharton T, Sarna T, Hamblin MR. Photodynamic therapy with fullerenes. Photochem Photobiol Sci 2007;6:1139–1149. [PubMed: 17973044]
20. Mroz P, Pawlak A, Satti M, Lee H, Wharton T, Gali H, et al. Functionalized fullerenes mediate photodynamic killing of cancer cells: Type I versus Type II photochemical mechanism. Free Radic Biol Med 2007;43:711–719. [PubMed: 17664135]
21. Yamakoshi Y, Umezawa N, Ryu A, Arakane K, Miyata N, Goda Y, et al. Active oxygen species generated from photoexcited fullerene (C60) as potential medicines: O2-* versus 1O2. J Am Chem Soc 2003;125:12803–12809. [PubMed: 14558828]
22. Zhao B, He YY, Bilski PJ, Chignell CF. Pristine (C60) and hydroxylated [C60(OH)24] fullerene phototoxicity towards HaCaT keratinocytes: type I vs type II mechanisms. Chem Res Toxicol 2008;21:1056–1063. [PubMed: 18422350]

23. Tegos GP, Demidova TN, Arcila-Lopez D, Lee H, Wharton T, Gali H, et al. Cationic fullerenes are effective and selective antimicrobial photosensitizers. Chem Biol 2005;12:1127–1135. [PubMed: 16242655]
24. Nobile CJ, Mitchell AP. Regulation of cell-surface genes and biofilm formation by the C. albicans transcription factor Bcr1p. Curr Biol 2005;15:1150–1155. [PubMed: 15964282]
25. Sherman F. Getting started with yeast. Methods Enzymol 1991;194:3–21. [PubMed: 2005794]
26. Demidova TN, Hamblin MR. Effect of cell-photosensitizer binding and cell density on microbial photoinactivation. Antimicrob Agents Chemother 2005;49:2329–2335. [PubMed: 15917529]
27. Jett BD, Hatter KL, Huycke MM, Gilmore MS. Simplified agar plate method for quantifying viable bacteria. Biotechniques 1997;23:648–650. [PubMed: 9343684]
28. Spesia MB, Milanesio ME, Durantini EN. Synthesis, properties and photodynamic inactivation of Escherichia coli by novel cationic fullerene C(60) derivatives. Eur J Med Chem. 2007
29. Maggini M, Scorrano G, Prato M. Addition Of Azomethine Ylides To C-60 -Synthesis, Characterization, And Functionalization Of Fullerene Pyrrolidines. J Am Chem Soc 1993;115:9798–9799.
30. Jafvert CT, Kulkarni PP. Buckminsterfullerene's (C60) octanol-water partition coefficient (Kow) and aqueous solubility. Environ Sci Technol 2008;42:5945–5950. [PubMed: 18767649]
31. Tegos GP, Demidova TN, Arcila-Lopez D, Lee H, Wharton T, Gali H, et al. Cationic fullerenes are effective and selective antimicrobial photosensitizers. Chem Biol 2005;12:1127–1135. [PubMed: 16242655]
32. Bakry R, Vallant RM, Najam-ul-Haq M, Rainer M, Szabo Z, Huck CW, et al. Medicinal applications of fullerenes. Int J Nanomedicine 2007;2:639–649. [PubMed: 18203430]
33. Demidova TN, Hamblin MR. Photodynamic therapy targeted to pathogens. Int J Immunopathol Pharmacol 2004;17:245–254. [PubMed: 15461858]
34. Gottenbos B, van der Mei HC, Klatter F, Grijpma DW, Feijen J, Nieuwenhuis P, et al. Positively charged biomaterials exert antimicrobial effects on gram-negative bacilli in rats. Biomaterials 2003;24:2707–2710. [PubMed: 12711516]
35. Mitik-Dineva N, Wang J, Truong VK, Stoddart P, Malherbe F, Crawford RJ, et al. Escherichia coli, Pseudomonas aeruginosa, and Staphylococcus aureus attachment patterns on glass surfaces with nanoscale roughness. Curr Microbiol 2009;58:268–273. [PubMed: 19020934]
36. Fass RJ, Barnishan J. Effect of divalent cation concentrations on the antibiotic susceptibilities of nonfermenters other than Pseudomonas aeruginosa. Antimicrob Agents Chemother 1979;16:434–438. [PubMed: 117746]
37. Vaara M. Agents that increase the permeability of the outer membrane. Microbiol Rev 1992;56:395–411. [PubMed: 1406489]
38. Hancock RE. The Pseudomonas aeruginosa outer membrane permeability barrier and how to overcome it. Antibiot Chemother 1985;36:95–102. [PubMed: 2988427]
39. Yoshimura F, Nikaido H. Permeability of Pseudomonas aeruginosa outer membrane to hydrophilic solutes. J Bacteriol 1982;152:636–642. [PubMed: 6813310]
40. Hancock RE. Resistance mechanisms in Pseudomonas aeruginosa and other nonfermentative gram-negative bacteria. Clin Infect Dis 1998;27:S93–99. [PubMed: 9710677]
41. George S, Hamblin MR, Kishen A. Uptake pathways of anionic and cationic photosensitizers into bacteria. Photochem Photobiol Sci 2009;8:788–795. [PubMed: 19492106]
42. Merchat M, Spikes JD, Bertoloni G, Jori G. Studies on the mechanism of bacteria photosensitization by meso-substituted cationic porphyrins. J Photochem Photobiol B 1996;35:149–157. [PubMed: 8933721]
43. Bliss JM, Bigelow CE, Foster TH, Haidaris CG. Susceptibility of Candida species to photodynamic effects of photofrin. Antimicrob Agents Chemother 2004;48:2000–2006. [PubMed: 15155191]
44. Munin E, Giroldo LM, Alves LP, Costa MS. Study of germ tube formation by Candida albicans after photodynamic antimicrobial chemotherapy (PACT). J Photochem Photobiol B 2007;88:16–20. [PubMed: 17566757]
45. Demidova TN, Hamblin MR. Effect of cell-photosensitizer binding and cell density on microbial photoinactivation. Antimicrob Agents Chemother 2005;49:2329–2335. [PubMed: 15917529]

46. Blanco MT, Blanco J, Sanchez-Benito R, Perez-Giraldo C, Moran FJ, Hurtado C, et al. Incubation temperatures affect adherence to plastic of Candida albicans by changing the cellular surface hydrophobicity. Microbios 1997;89:23–28. [PubMed: 9254331]
47. Hazen KC, Brawner DL, Riesselman MH, Jutila MA, Cutler JE. Differential adherence of hydrophobic and hydrophilic Candida albicans yeast cells to mouse tissues. Infect Immun 1991;59:907–912. [PubMed: 1900065]
48. Soukos NS, Ximenez-Fyvie LA, Hamblin MR, Socransky SS, Hasan T. Targeted antimicrobial photochemotherapy. Antimicrob Agents Chemother 1998;42:2595–2601. [PubMed: 9756761]
49. Soukos NS, Wilson M, Burns T, Speight PM. Photodynamic effects of toluidine blue on human oral keratinocytes and fibroblasts and Streptococcus sanguis evaluated in vitro. Lasers Surg Med 1996;18:253–259. [PubMed: 8778520]
50. Zeina B, Greenman J, Corry D, Purcell WM. Cytotoxic effects of antimicrobial photodynamic therapy on keratinocytes in vitro. Br J Dermatol 2002;146:568–573. [PubMed: 11966685]

List of Abbreviations

BF	buckminsterfullerene
BHI	brain heart infusion
CFU	colony forming units
DMSO	dimethylsulfoxide
ESI-MS	electro-spray ionization mass spectrometry
FTIR	Fourier transform infra red (spectroscopy)
MALDI TOF-MS	matrix assisted laser desorption ionization; time of flight; mass spectrometry
NAD(P)H	nicotinamide adenine dinucleotide reduced form
PBS	phosphate buffered saline
PDI	photodynamic inactivation
PDT	photodynamic therapy
PS	photosensitizer
ROS	reactive oxygen species
YPD	yeast potato dextrose

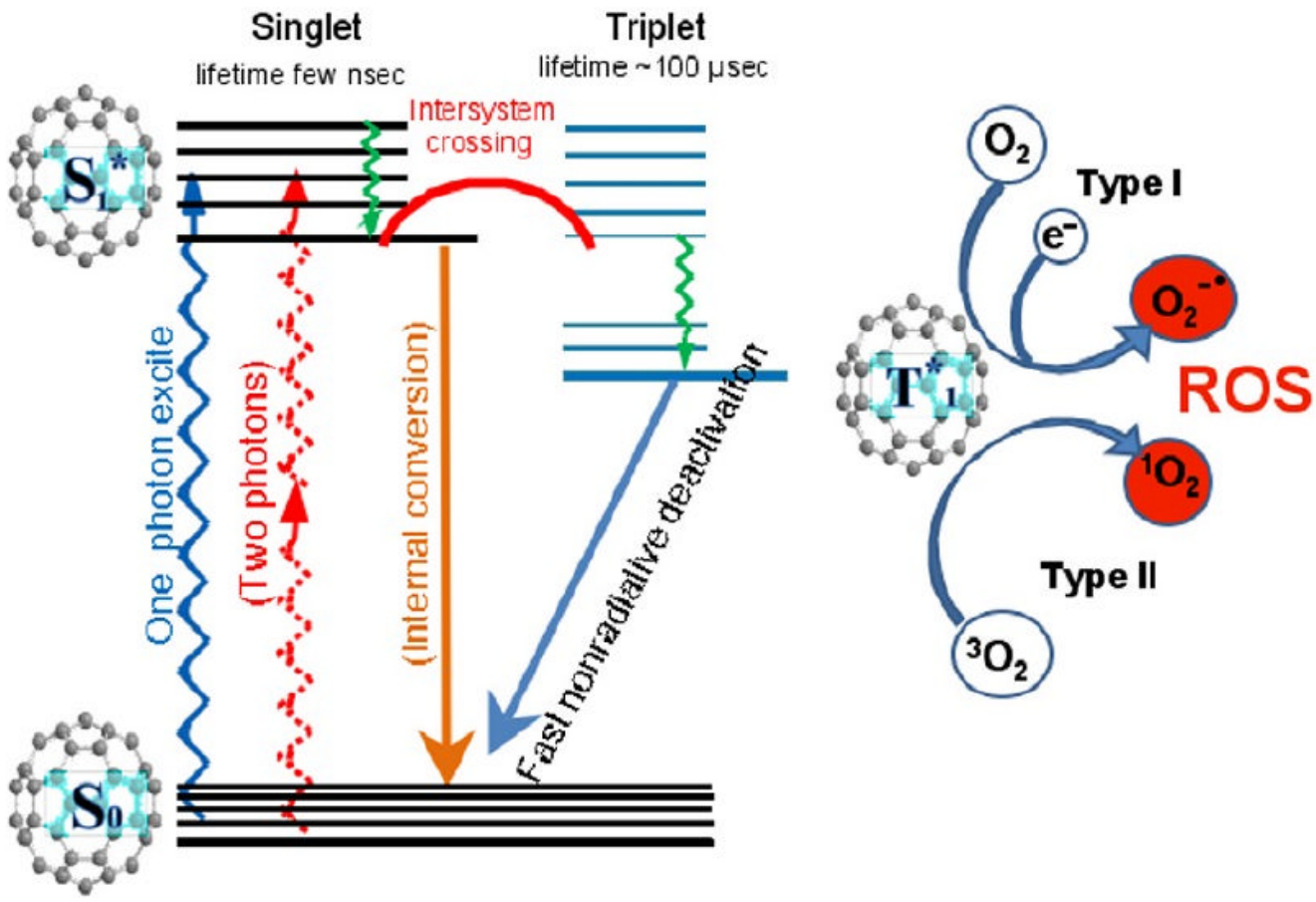

Figure 1.
Schematic illustration of fullerene-mediated photodynamic therapy including the Jablonski diagram and the formation of Type I and Type II reactive oxygen species.

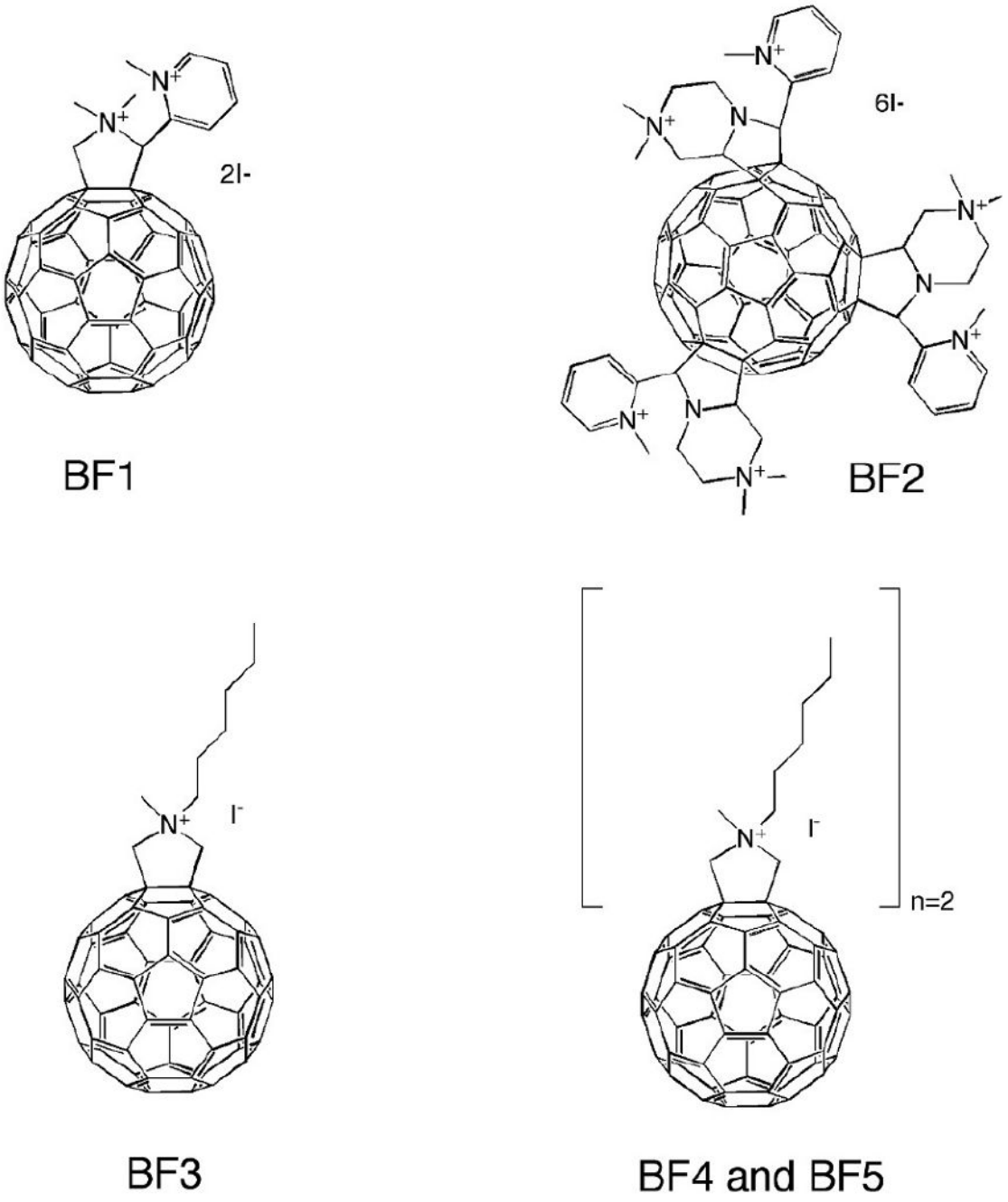

Figure 2.
Structural formulas of the fullerenes studied in this report. Note that **BF2** is a mixture of bis- (not shown) and tris- (shown) substituted fullerenes.

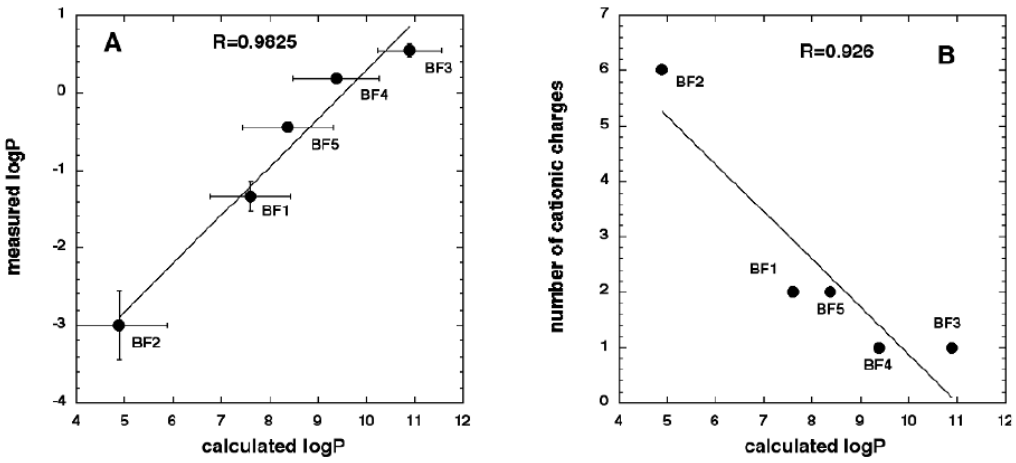

Figure 3.
(A) Linear correlation between measured and calculated logP values. (B) Linear correlation between calculated logP values and number of cationic charges.

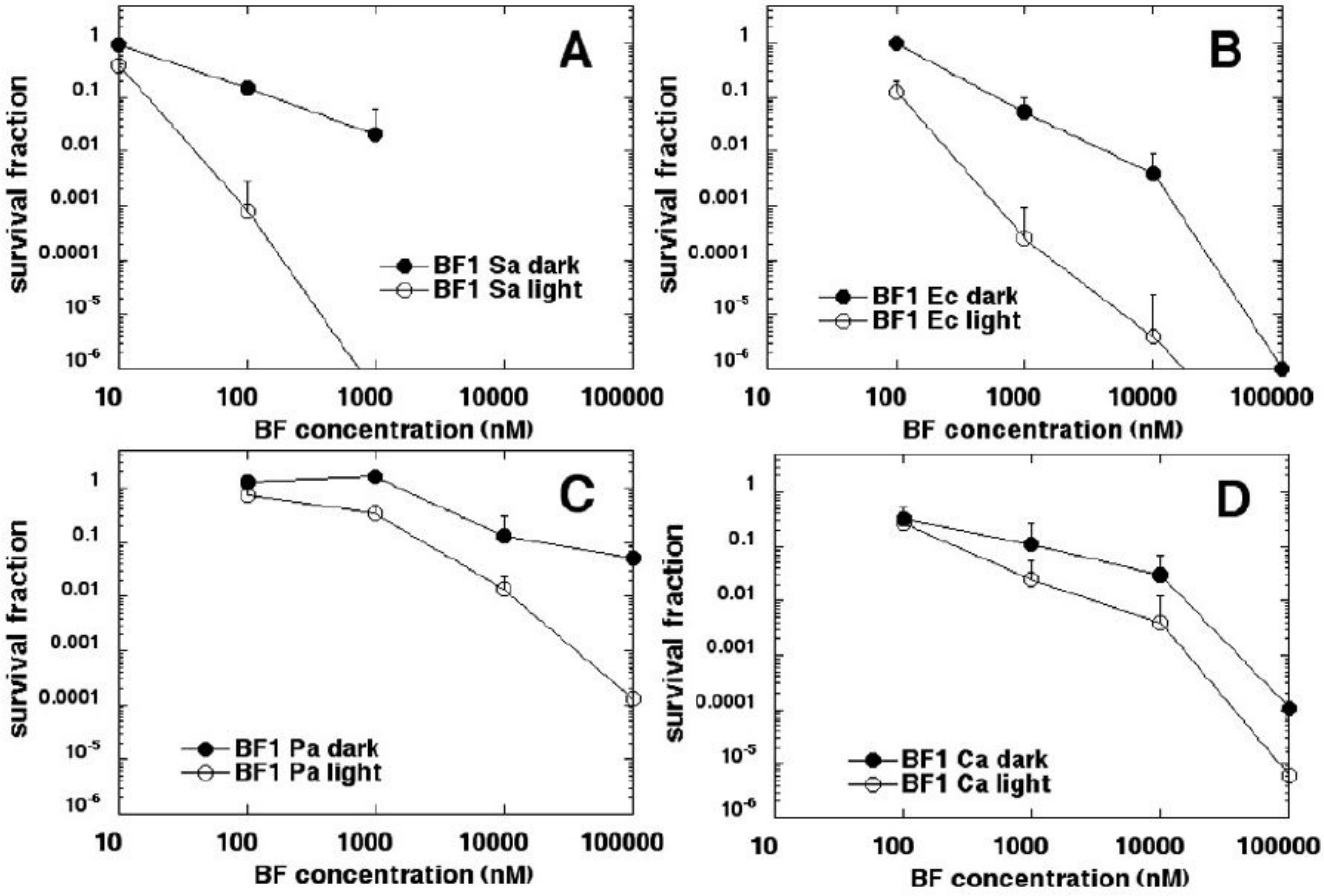

Figure 4.

Killing curves for microbial cells with increasing concentrations of **BF1** in dark and after illumination with 10 J/cm2 of 400-700-nm white light. (A) *S. aureus*; (B) *E. coli*; (C) *P. aeruginosa*; (D) *C. albicans*. Plots shown are representative of three repetitions.

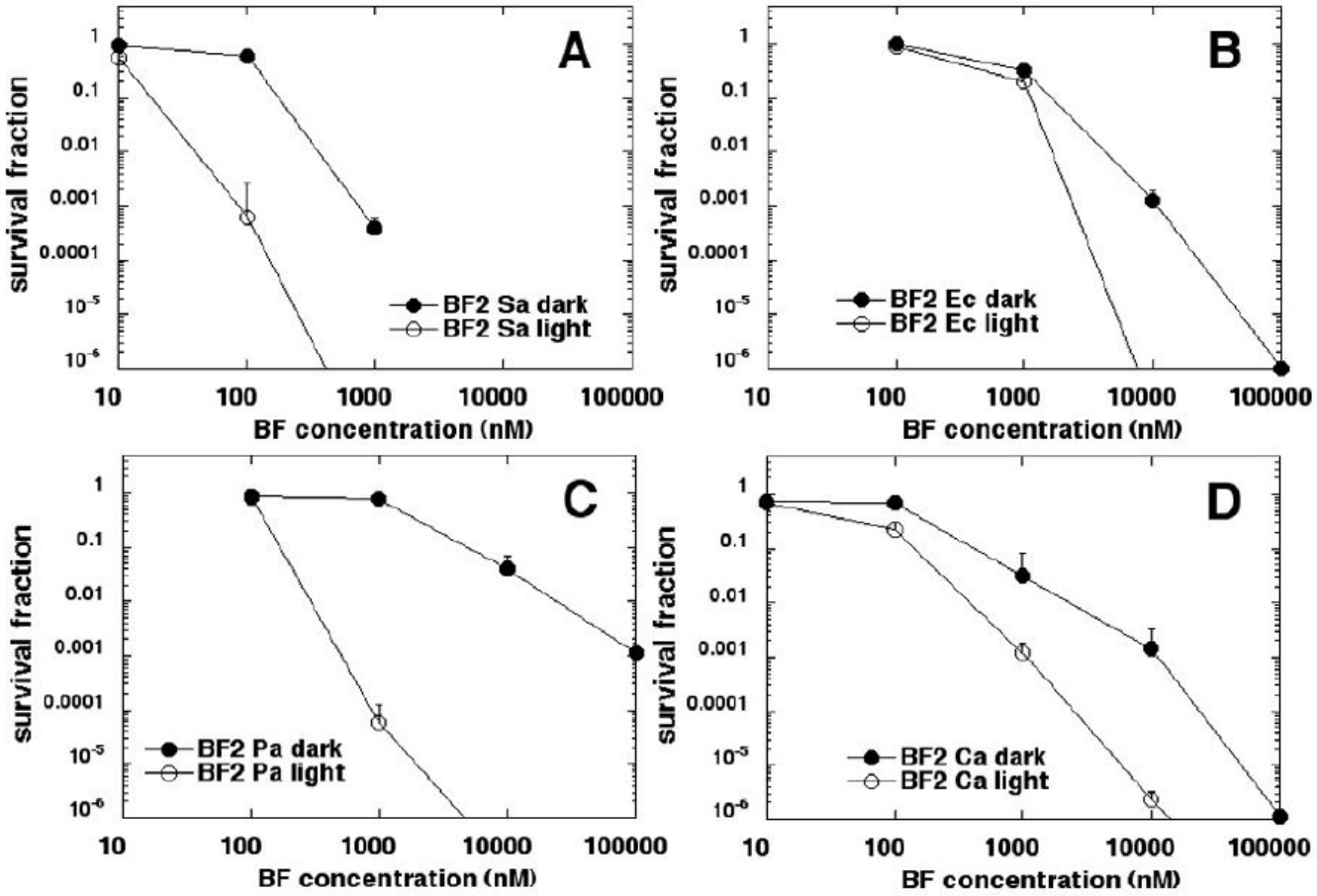

Figure 5.

Killing curves for microbial cells with increasing concentrations of **BF2** in dark and after illumination with 10 J/cm2 of 400-700-nm white light. (A) *S. aureus*; (B) *E. coli*; (C) *P. aeruginosa*; (D) *C. albicans*. Plots shown are representative of three repetitions.

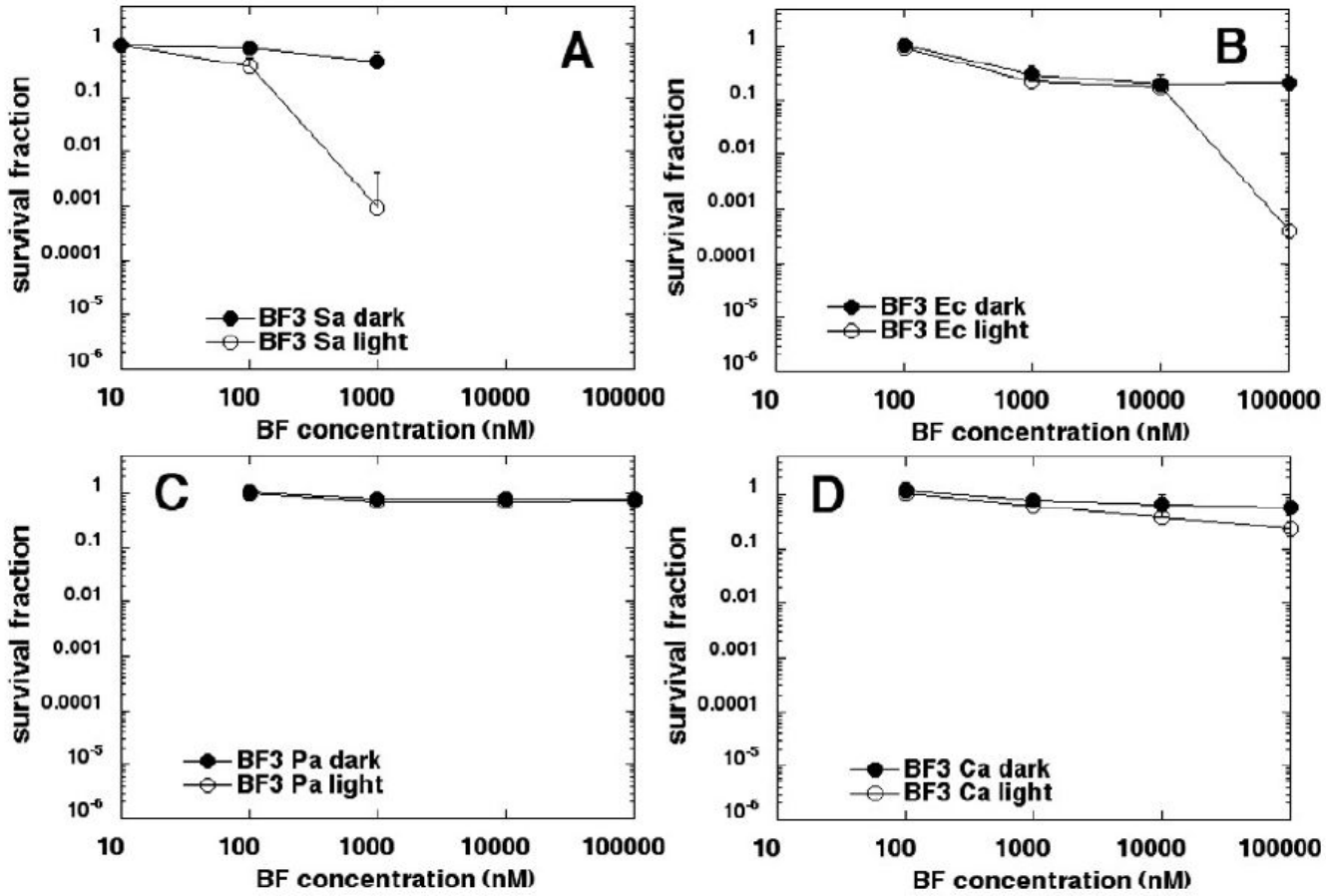

Figure 6.

Killing curves for microbial cells with increasing concentrations of **BF3** in dark and after illumination with 10 J/cm2 of 400-700-nm white light. (A) *S. aureus*; (B) *E. coli*; (C) *P. aeruginosa*; (D) *C. albicans*. Plots shown are representative of three repetitions.

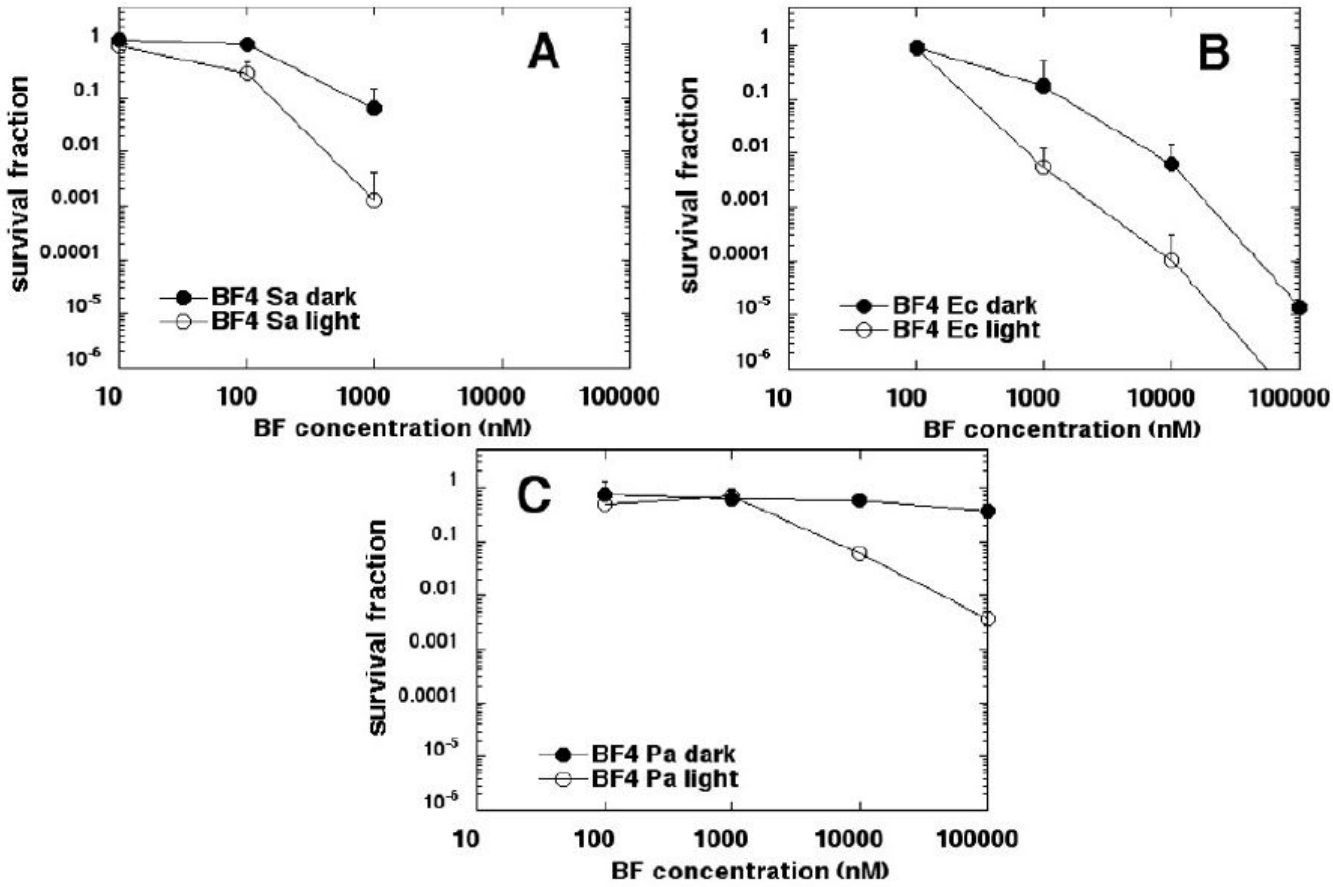

Figure 7.

Killing curves for microbial cells with increasing concentrations of **BF4** in dark and after illumination with 10 J/cm2 of 400-700-nm white light. (A) *S. aureus*; (B) *E. coli*; (C) *P. aeruginosa*. Plots shown are representative of three repetitions.

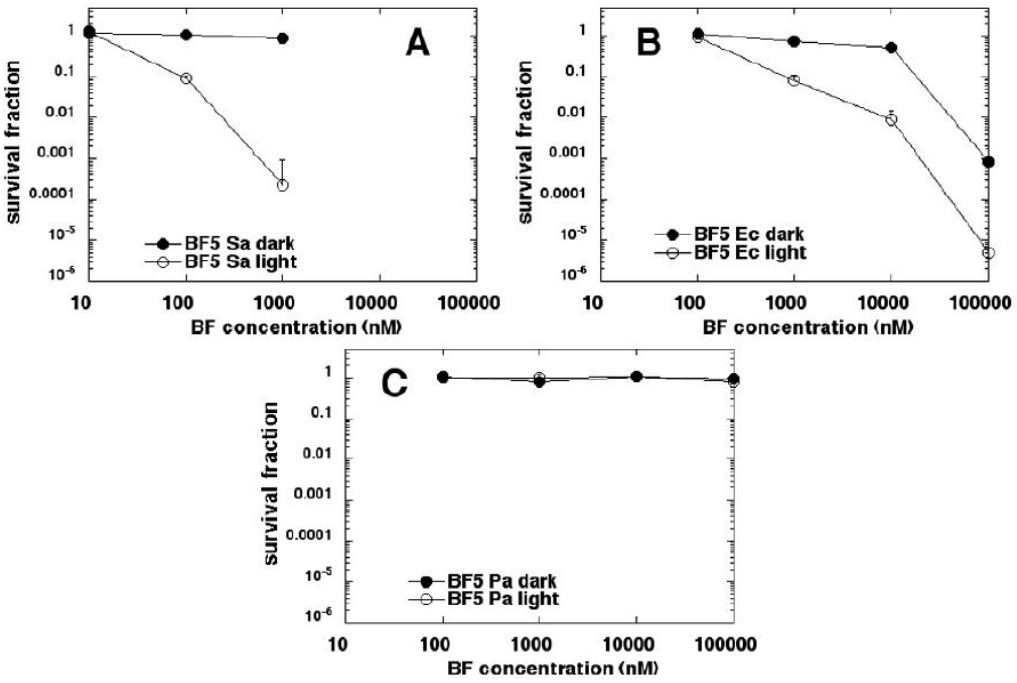

Figure 8.

Killing curves for microbial cells with increasing concentrations of **BF5** in dark and after illumination with 10 J/cm2 of 400-700-nm white light. (A) *S. aureus*; (B) *E. coli*; (C) *P. aeruginosa*. Plots shown are representative of three repetitions.

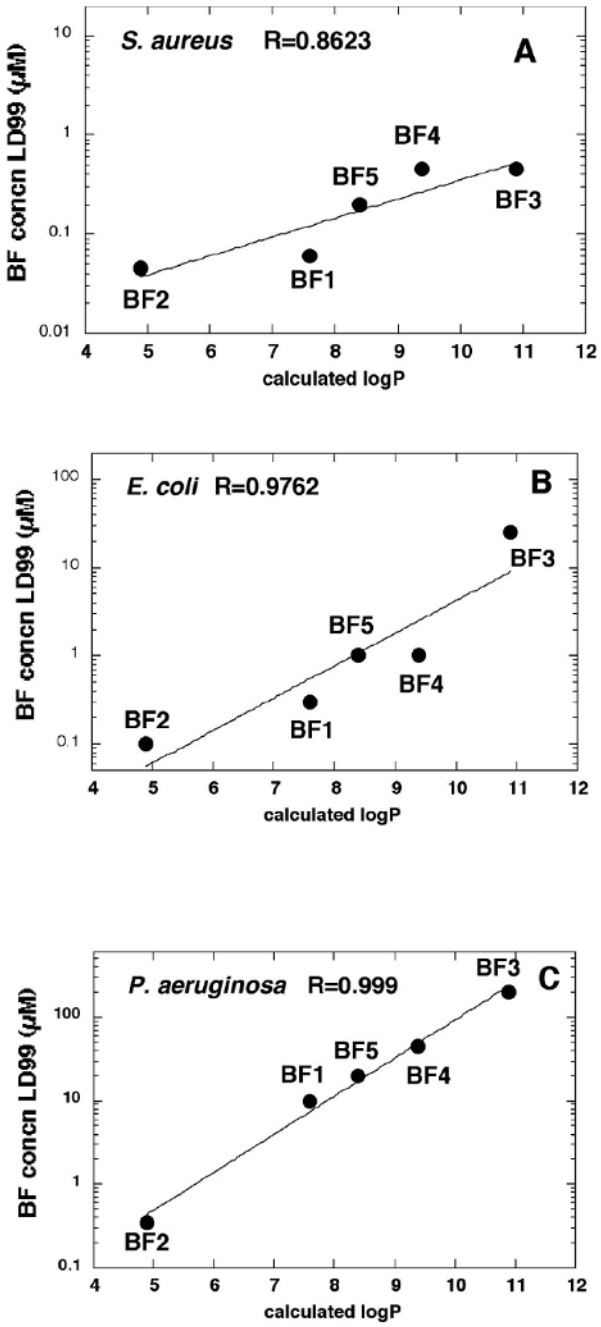

Figure 9.

Linear correlation plots between the concentration of fullerene need to kill 99% of cells after illumination (LD99) and calculated logP values. (A) *S. aureus*; (B) *E. coli*; (C) *P. aeruginosa*.